Int. J. Heat Mass Transfer. Vol. 24, No. 8, pp. 1369–1379, 1981.
Printed in Great Britain

0017-9310/81/081369-11 $02.00/0
Pergamon Press Ltd.

NUMERICAL SOLUTION OF STEADY-STATE FREE CONVECTIVE HEAT TRANSFER FROM A SOLID SPHERE

F. GEOOLA

Materials and Energy Research Centre (MERC), Sharif University of Technology, P.O. Box 41-2927 Tehran, Iran

and

A. R. H. CORNISH

Chemical Engineering Department, Imperial College of Science and Technology, Prince Consort Road, London S.W.7, U.K.

(*Received* 18 *December* 1979 *and in revised form* 26 *January* 1981)

Abstract—A numerical study has been made of steady-state free convective heat transfer from a solid sphere to an incompressible Newtonian fluid for Grashof numbers of 0.05, 1, 10, 25 and 50 for a Prandtl number of 0.72. The stream function, energy, and vorticity transport equations were solved using an extrapolated Gauss– Seidel method. The values obtained for the average Nusselt number were found to be in reasonable agreement with the experimental measurements obtained by previous workers. It was also observed that the method used could not be applied to find solutions for Grashof numbers greater than 50.

NOMENCLATURE

C_{DF}, dimensionless viscous drag;
C_{DP}, dimensionless pressure drag;
C_{DT}, dimensionless total drag;
C_p, specific heat at constant pressure;
G, modified dimensionless vorticity defined by equation (6);
Gr, Grashof number based on the radius of the sphere $(R^3\beta g(T_s - T_\infty)/\nu^2)$;
g, gravitational acceleration;
h, average heat transfer coefficient;
h_θ, local heat transfer coefficient;
K_0, dimensionless pressure at the front stagnation point;
K_θ, dimensionless pressure at sphere surface;
k, thermal conductivity;
M, number of mesh points in the z-direction;
m, mesh size in the z-direction;
N, number of mesh points in the θ-direction;
n, mesh size in the θ-direction;
Nu, average Nusselt number $(2RH/k)$;
Nu_θ, local Nusselt number $(2Rh_\theta/k)$;
Pr, Prandtl number (ν/α);
R, radius of sphere;
Ra, Rayleigh number $(GrPr)$;
r, dimensionless radial coordinate;
(r, θ, ϕ), spherical polar coordinates;
T, dimensionless temperature;
u_z, u_θ, dimensionless velocity components in the z and θ-directions;
W, a general continuous function representing T, G and ψ;
y_1, y_2, y_3, rectangular cartesian coordinates;
z, modified coordinate defined as $z = \ln r$.

Greek symbols

α, thermal diffusivity $(k/\rho C_p)$;
β, volumetric coefficient of expansion with temperature;
ε_G, convergence criterion for the vorticity;
ε_T, convergence criterion for the temperature;
ε_W, convergence criterion for a general function;
ε_ψ, convergence criterion for the stream function;
ζ, dimensionless vorticity component in the ϕ-direction;
θ, angular coordinate;
ν, fluid kinematic viscosity;
ρ, density;
ϕ, coordinate representing the angle of rotation about the axis of symmetry of the flow;
ψ, dimensionless stream function;
ω_G, relaxation factor for the vorticity;
ω_T, relaxation factor for the temperature;
ω_W, relaxation factor for a general function;
ω_z, weighting factor for upwind difference representation of a first-order derivative with respect to z;
ω_θ, weighting factor for upwind difference representation of a first-order derivative with respect to θ;
ω_ψ, relaxation factor for the stream function.

Subscripts

i, mesh point index in the z-direction;
j, mesh point index in the θ-direction;

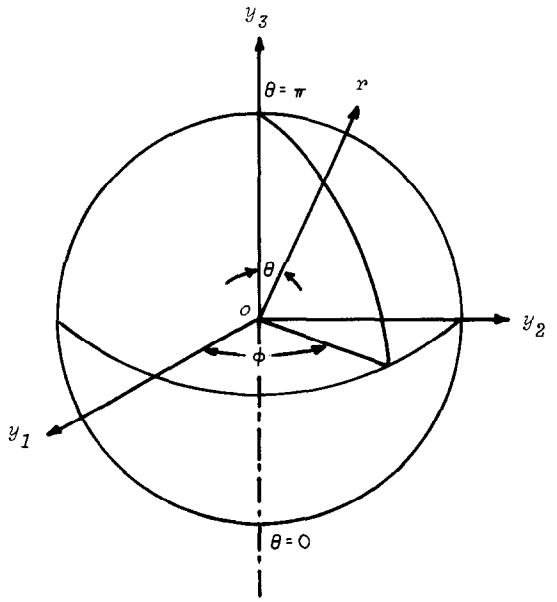

FIG. 1. Spherical polar coordinate system.

i,j, indices of a mesh point in the flow region;
s, sphere surface;
∞, outer boundary condition.

Superscripts
(L), (L)th iteration;
$(L-1)$, $(L-1)$th iteration.

1. INTRODUCTION

THE PROCESS of heat transfer by free convection is encountered frequently in industrial applications such as steam boilers, digesters, furnaces, etc. In general, free convective heat transfer becomes an important mode of heat transfer in any situation in which a hot body is immersed in an otherwise stationary medium.

Because of its considerable importance in many engineering applications the fundamentals of heat and mass transfer from solid particles, drops, or bubbles to a continuous fluid phase have long attracted the attention of investigators. The study of heat transfer from a single sphere together with the associated fluid dynamics has been used as a first step in the analysis of multiparticle systems.

A considerable number of experimental and theoretical studies have been carried out on free convective heat and mass transfer from spherical particles at high Rayleigh numbers ($Ra > 10^5$, see for example Pandya [1]). However, relatively few workers have studied the same problem at low Rayleigh numbers possibly because of the experimental difficulties involved and because boundary layer theory is not applicable. Thus, theoretical work has to be based on numerical solutions of the Navier–Stokes and energy equations.

The pertinent analytical and experimental studies of free convective heat transfer from a sphere are the analytical studies of Mahony [2] and Fendel [3], and the analytical and experimental study of Hossain [4], and the experimental works of Meyer [5], Elenbaas [6], Ranz and Marshall [7], Mathers, Madden and Piret [8], Tsubouchi and Sato [9] and Yuge [10]. Most of these studies were confined to the determination of average Nusselt numbers. Hossain [4] was the only one who obtained flow patterns and temperature distributions about a sphere and he was only able to obtain them for extremely small Grashof numbers ($Gr \leq 1.0$). There have been no reports of complete analytical or numerical solutions for Grashof numbers larger than 1.0.

The axially symmetric nature of the problem enabled the Navier–Stokes and the continuity equations to be combined and expressed as a vorticity transport equation and a stream function equation. These latter two and the energy equation were solved simultaneously.

For purpose of computation, the elliptic second-order partial differential equations were replaced by the appropriate finite-difference approximations in which an upwind differencing scheme was applied to the convective terms of the transport equations.

2. THEORETICAL ANALYSIS

The geometry considered consisted of a heated solid sphere immersed in a fluid enclosed in a concentric spherical shell of uniform and unchanging temperature.

To obtain the flow and temperature distributions the Navier–Stokes, continuity and energy equations were expressed in spherical polar coordinates. The spherical polar coordinates (r, θ, ϕ) of the sphere are arranged as shown in Fig. 1. As shown in the figure, the coordinate r is normal to the surface of the body, θ is parallel to the surface in the flow direction and ϕ is the direction of rotation about the axis of symmetry of the flow. For the particular case of streaming flow past a stationary sphere with no rotation, the flow around the vertical axis is axisymmetric, the component of velocity in the ϕ-direction is zero everywhere, and all variables are independent of ϕ.

The Navier–Stokes and continuity equations were combined and expressed in the form of a stream function and a vorticity transport equation set. The vorticity, which is the curl of velocity in a fluid, is a vector quantity having the same nature as angular velocity. From the definition of the vorticity vector and from the condition of axisymmetrical flow, there is only one non-zero component of vorticity, that is in the ϕ-direction. The derivation of vorticity and stream function equation set from the Navier Stokes and continuity equations may be found in Batchelor [11].

Numerical solutions of the energy, vorticity transport and stream function equations can be obtained more conveniently if the equations are expressed in

dimensionless form. In view of this the variables have been rendered dimensionless with reference to the radius of the sphere, the kinematic viscosity of the fluid at the temperature of the outer boundary (ν_∞), and the temperature difference between the sphere surface and the outer boundary. It was also convenient to transform the equations from polar coordinates (r, θ) to rectangular coordinates (z, θ) by means of the transformation of $r = e^z$. The dimensionless system of the equations in rectangular coordinates (z, θ) can be written as follows:

The velocity components

$$u_z = -\frac{1}{e^{2z}\sin\theta}\frac{\partial\psi}{\partial\theta} \tag{1}$$

$$u_\theta = \frac{1}{e^{2z}\sin\theta}\frac{\partial\psi}{\partial z}. \tag{2}$$

The energy equation

$$\frac{1}{e^z\sin\theta}\left(\frac{\partial\psi}{\partial z}\frac{\partial T}{\partial\theta} - \frac{\partial\psi}{\partial\theta}\frac{\partial T}{\partial z}\right) = \frac{1}{Pr}\left(\frac{\partial^2 T}{\partial z^2} + \frac{\partial T}{\partial z} + \frac{\partial^2 T}{\partial\theta^2} + \cot\theta\frac{\partial T}{\partial\theta}\right). \tag{3}$$

The vorticity transport equation

$$\frac{1}{e^z\sin\theta}\left[\frac{\partial\psi}{\partial z}\left(\frac{\partial G}{\partial\theta} - 2\cot\theta G\right) - \frac{\partial\psi}{\partial\theta}\left(\frac{\partial G}{\partial z} - 2G\right)\right] = e^{2z}E^2(G) + e^{2z}\sin^2\theta Gr\left(\frac{\partial T}{\partial z} + \cot\theta\frac{\partial T}{\partial\theta}\right). \tag{4}$$

The stream function equation

$$e^{2z}G = e^{2z}E^2(\psi) \tag{5}$$

where

$$G = \zeta^z\sin\theta \tag{6}$$

and

$$e^{2z}E^2 = \frac{\partial^2}{\partial z^2} - \frac{\partial}{\partial z} + \frac{\partial^2}{\partial\theta^2} - \cot\theta\frac{\partial}{\partial\theta}. \tag{7}$$

Equations (1)–(7) are dependent upon the assumptions that the only body force operating is that of gravity and that temperature variations within the fluid are not large, so that Boussinesq's approximation can be applied thus enabling the density to be treated as a constant in all terms of the transport equations except the buoyancy term. Other fluid properties such as the viscosity, specific heat, and thermal conductivity are taken to be constant.

Equations (1)–(7) are subject to the following boundary conditions.

Sphere surface: on the sphere surface the 'no slip' condition is applied. Therefore, at $z = 0$ for $0 \le \theta \le \pi$

$$\psi = 0;\quad \frac{\partial\psi}{\partial z} = 0;\quad \frac{\partial\psi}{\partial\theta} = 0;\quad \frac{\partial^2\psi}{\partial\theta^2} = 0$$

$$G = \zeta\sin\theta = \frac{\partial^2\psi}{\partial z^2};\quad T = 1. \tag{8}$$

Axis of symmetry: along the axis of symmetry ($\theta = 0$ and $\theta = \pi$), the 'no cross flow' condition is applied. Therefore, at $\theta = 0$ and $\theta = \pi$ for all values of z

$$\psi = 0;\quad \frac{\partial\psi}{\partial z} = 0;\quad \frac{\partial^2\psi}{\partial z^2} = 0;$$

$$\frac{\partial\psi}{\partial\theta} = 0;\quad G = 0;\quad \frac{\partial T}{\partial\theta} = 0. \tag{9}$$

Outer boundary: conditions at the outer boundary are only well defined when the outer boundary radius tends to infinity; however, because of limitations of computer storage and computation time a finite domain of integration has to be used and it is considered that at a finite but large radius, all the dependent variables become asymptotic to their values in the undisturbed stagnant fluid. Therefore at $z = z_\infty$ for $0 \le \theta \le \pi$

$$\psi = 0;\quad G = 0;\quad \zeta = 0;\quad T = 0. \tag{10}$$

From the distribution of stream function, vorticity and temperature other quantities can be calculated as follows.

Local Nusselt number at the sphere surface

$$Nu_\theta = -2\left.\frac{\partial T}{\partial z}\right|_{z=0}. \tag{11}$$

Average or overall Nusselt number

$$Nu = \frac{1}{2}\int_0^\pi Nu_\theta\sin\theta\,d\theta. \tag{12}$$

Dimensionless pressure at the front stagnation point

$$K_0 = 4\int_0^{z_\infty}\frac{\partial\zeta}{\partial\theta}dz + 2Gr\int_0^{z_\infty} T\,e^z\,dz. \tag{13}$$

Dimensionless pressure at the sphere surface (surface pressure)

$$K_\theta = K_0 + 2Gr(1-\cos\theta) + 2\int_0^\theta\left(\frac{\partial\zeta}{\partial z} + \zeta\right)d\theta. \tag{14}$$

Dimensionless pressure drag (form drag)

$$C_{DP} = \int_0^\pi K_\theta\sin 2\theta\,d\theta. \tag{15}$$

Dimensionless viscous drag (frictional drag)

$$C_{DF} = 4\int_0^\pi \zeta_s\sin^2\theta\,d\theta. \tag{16}$$

Dimensionless total drag

$$C_{DT} = C_{DP} + C_{DF}. \tag{17}$$

The integrands in equations (13) and (14) were evaluated at $\theta = 0$ and at $z = 0$, respectively.

3. NUMERICAL METHOD

The set of differential equations and boundary conditions, presented in Section 2, were solved numerically. The first step in the solution of the equations by a

finite-difference method is to reduce them from continuous to discrete forms and then to solve the resulting algebraic equations on a digital computer.

The basic method is to expand the terms of the original partial differential equations in Taylor's series. The series are truncated to a reasonable accuracy and a set of finite-difference equations obtained by the replacement of each term by the truncated series. Each finite-difference equation relates the value of a function at any mesh point to the values at neighbouring mesh points. In the present work a five point approximation, involving four neighbouring points, has been used. The details of the method used can be found in Smith [12], Richtmyer and Morton [13] and Roache [14].

The coordinates z and θ introduced in previous sections form a rectangular system of coordinates. The domain over which the equations were to be integrated, the flow region, was represented by a finite number of points spaced systematically within the domain. The mesh points were spaced uniformly in both the z and θ-directions.

The vorticity, temperature and stream function equations were solved using an extrapolated Gauss–Seidel method. The method was basically the same as the simple Gauss–Seidel iterative method [12]. However, in order to accelerate the rate of convergence, a relaxation factor, ω_W, which has a value between 0.0 and 2.0 was introduced into the finite-difference equations as follows:

$$W_{i,j}^{(L)} = W_{i,j}^{(L-1)} + \omega_W R_{i,j}^{(L)} \tag{18}$$

where the function W, can be either the temperature, T, the vorticity, G, or the stream function, ψ and $R_{i,j}^{(L)}$ is the amount by which the values of $W_{i,j}^{(L)}$ change for one iteration. At complete convergence, $R_{i,j}^{(L)}$ is equal to zero. In this work, the following convergence criterion was used

$$|W_{i,j}^{(L)} - W_{i,j}^{(L-1)}| \leq \varepsilon_W. \tag{19}$$

Soo [15] has explained the extrapolated Gauss–Seidel method in detail and shows that this method is a powerful tool for numerical solutions of nonlinear elliptic partial differential equations.

Numerical experimentation revealed that it was not possible to use a central difference scheme which was stable over the entire space region of interest. Hellums [16] came to the same conclusion for free convective problems. This problem is closely related to the concept of a 'transportive property' which is well explained by Roache [14]. In the present work, in order to preserve the transportive property and to obtain stability and convergence an upwind differencing method was used for the finite-difference representation of the convective terms of the equations. In this scheme the terms in which the velocity components appear as coefficients, the convective terms were approximated by backward differences when the velocity coefficients were positive. Forward differences, therefore, were used when the velocity coefficients were negative. This was achieved by the use of weighting factors ω_z and ω_θ in the upwind differences of the first order derivatives in the convective terms.

As an example of the scheme used, the finite-difference approximation of the vorticity transport equation is presented as follows:

$$\begin{aligned}
&\frac{\Delta_i(\psi_{ij})}{2mn\,e^{2i}\sin\theta_j}[\omega_\theta G_{i,j+1} + (1-2\omega_\theta)G_{i,j} \\
&\quad -(1-\omega_\theta)G_{i,j-1} - 2n\cot\theta_j G_{i,j}] \\
&\quad -\frac{\Delta_j(\psi_{ij})}{2mn\,e^{2i}\sin\theta_j}[\omega_z G_{i+1,j} + (1-2\omega_z)G_{i,j} \\
&\quad -(1-\omega_z)G_{i-1,j} - 2mG_{i,j}] \\
&= \left(\frac{1}{m^2} - \frac{1}{2m}\right)G_{i+1,j} + \left(\frac{1}{m^2} + \frac{1}{2m}\right)G_{i-1,j} \\
&\quad + \left(\frac{1}{n^2} - \frac{\cot\theta_j}{2n}\right)G_{i,j+1} \\
&\quad + \left(\frac{1}{n^2} + \frac{\cot\theta_j}{2n}\right)G_{i,j-1} - \left(\frac{2}{m^2} + \frac{2}{n^2}\right)G_{i,j} \\
&\quad + \frac{e^{2i}\sin^2\theta_j Gr}{2mn}[n(T_{i+1,j} - T_{i-1,j}) \\
&\quad + m\cot\theta_j(T_{i,j+1} - T_{i,j-1})]
\end{aligned} \tag{20}$$

where

$$\Delta_i(\psi_{ij}) = \psi_{i+1,j} - \psi_{i-1,j} \tag{21}$$

and

$$\Delta_j(\psi_{ij}) = \psi_{i,j+1} - \psi_{i,j-1}. \tag{22}$$

Introduction of the weighting factors ω_z and ω_θ in equation (20) enabled four separate systems of finite-difference equations to be used in the approximation of the convective terms corresponding to the combinations of signs of the coefficients of the derivatives (velocities), in the convective terms.

The values of the weighting factors ω_z and ω_θ in equation (20) were determined in accordance with the signs of the coefficient $[-\Delta_j(\psi_{ij})]$ and $\Delta_i(\psi_{ij})$, respectively. When these coefficients were positive the weighting factors were set equal to zero (backward differences). However, when the coefficients were negative the weighting factors were set equal to one (forward differences). In this way the upwind differencing method was used in this study.

From a formal examination of the Taylor's series expansions of the convective terms of the equations it may be concluded that a central difference scheme is more accurate than upwind difference schemes. A particular kind of truncation error is associated with the application of upwind differencing schemes which is usually called 'false viscosity' (Roache [14] and Rafique [17]). Arguments have been made to the effect that accurate solutions are not possible unless the false viscosity introduced is much less than the real viscosity of the fluid [17]. However, the solutions obtained by other authors, as surveyed by Roache [14], for multi-

Table 1. Main results of this study for different Grashof numbers

Gr	0.05	1	10	25	50
m	0.04	0.04	0.04	0.04	0.03
n	6°	6°	6°	6°	6°
M	80	80	80	80	107
N	30	30	30	30	60
ω_G	1.2	1.2	1	0.8	0.5
ω_T	1.5	1.5	1.3	1.1	0.9
ω_ψ	1.3	1.2	1	0.9	0.7
ε_G	10^{-3}	10^{-3}	5×10^{-3}	10^{-2}	5×10^{-2}
ε_T	10^{-5}	10^{-5}	10^{-4}	5×10^{-4}	10^{-3}
ε_ψ	10^{-4}	10^{-4}	5×10^{-4}	10^{-3}	5×10^{-3}
Nu	2.09	2.39	2.96	3.32	3.96
K_0	0.50	5.97	36.07	76.23	118.30
K_π	−0.40	−5.40	−31.26	−48.69	−12.66
C_{DF}	1.17	16.42	74.88	143.70	211.20
C_{DP}	0.58	7.58	71.29	87.08	105.45

dimensional problems support the use of upwind difference schemes, in particular in the case of steady state problems. Furthermore, upwind difference schemes are used because they ensure stability and rapid convergence; with this in mind, the reduced accuracy may seem to be an acceptable penalty (Spalding, Gosman and Caretto [18] and Gosman *et al.* [19]).

The main sources of error which could have affected the accuracy of the results obtained in this study and the main factors which influenced the computation time were size of mesh spacing, proximity of the outer boundary, orders of the polynomials used to approximate the boundary conditions, convergence criteria and associated relaxation factors. Values for these factors were found on the basis of numerical experiments, and were selected in order to achieve a balance between accuracy and economy of the use of computing facilities.

At Grashof number less than 10 of the solutions converged rapidly and smoothly. However, at Grashof numbers greater than 10, vorticity fluctuations appeared close to the outer boundary. These fluctuations have been recorded by other workers (see for example, Soo [15] and Rafique [17]). It is generally known, however, that as long as the magnitude of the fluctuations is relatively small, it is unlikely that the solution, and, in particular, the derived flow characteristics close to the sphere surface will be affected [17]. Numerical experimentation, in the present work, revealed that the magnitude of the fluctuations for Grashof numbers less than 50 has not been large enough to affect the flow characteristics close to the sphere surface and therefore no attempt was made to cure the fluctuations. However, in the solutions obtained for a Grashof number of 50 the surface vorticity and as a consequence, the surface pressure and the drag coefficients were slightly affected by the fluctuations of the vorticity at the outer boundary. To obtain solutions at a Grashof number of 50, it was necessary to reduce the values of the mesh sizes and relaxation factors and to increase the values of the convergence criteria. At Grashof numbers greater than 50 the fluctuations became large and were propagated throughout the entire region of integration so that solutions could not be obtained.

The values of mesh sizes, relaxation factors, convergence criteria, and the number of mesh points used for different Grashof numbers are given in Table 1.

The average central processor time required to obtain a solution for Grashof numbers of 0.05 to 1 was found to be about 1 h, for Grashof numbers between 1 and 25 it was found to be about 3 h and for Grashof numbers between 25 and 50 it was found to be about 4 h when using a CDC6400 digital computer.

4. DISCUSSION OF RESULTS

Solutions were obtained for Grashof numbers of 0.05, 1, 10, 25 and 50 for a Prandtl number of 0.72. The main results are presented in terms of dimensionless variables in Table 1. In the contour drawings Figs. 2–7, the direction of flow along the axis of symmetry is from right ($\theta = 0$) to left ($\theta = \pi$).

Figures 2 and 3 show the distribution of the stream function at Grashof numbers of 0.05 and 25. As expected, the figures show that the rising and descending currents generate a circulatory flow pattern. As the

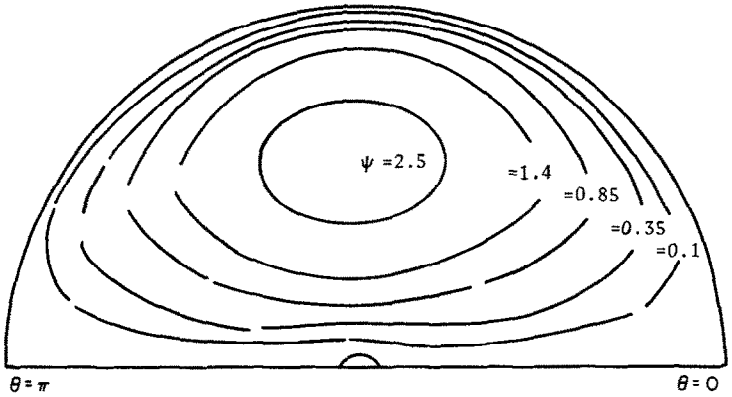

FIG. 2. Streamlines, $Gr = 0.05$, $Pr = 0.72$.

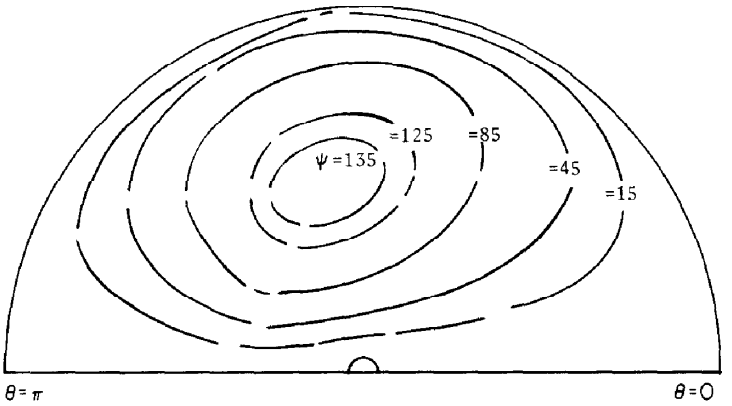

FIG. 3. Streamlines, $Gr = 25$, $Pr = 0.72$.

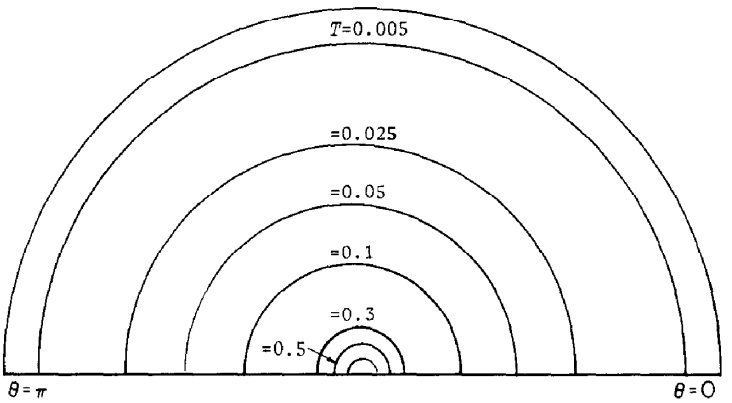

FIG. 4. Isotherms, $Gr = 0.05$, $Pr = 0.72$.

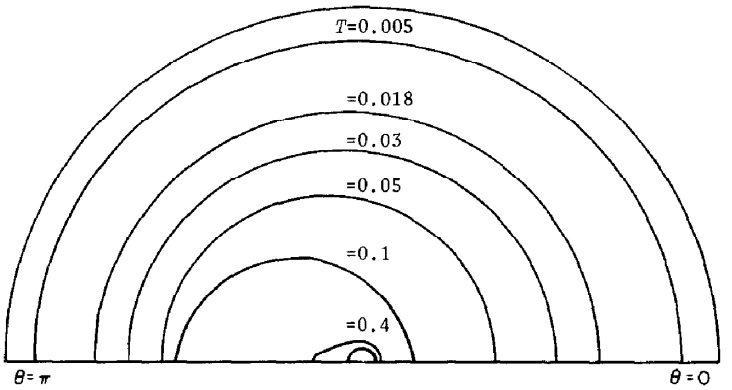

FIG. 5. Isotherms, $Gr = 25$, $Pr = 0.72$.

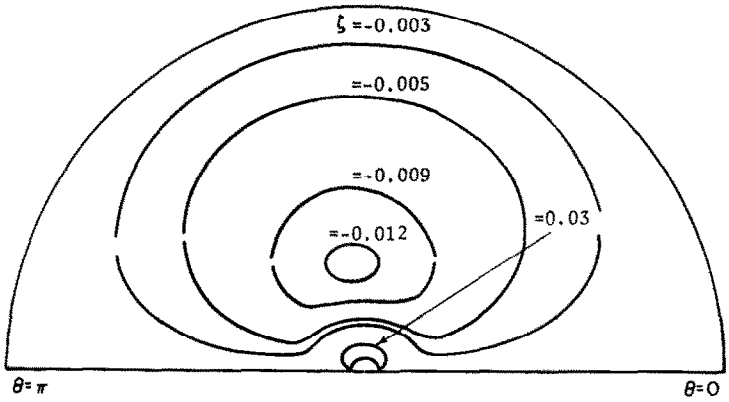

FIG. 6. Vorticity distribution, $Gr = 0.05$, $Pr = 0.72$.

Grashof number increases the stream function contours move downstream. This is because as the Grashof number increases, the ratio of the buoyancy forces to the viscous forces increases, thus increasing the effects of convection and the rate of heat transfer. As a result, the thickness of the heated layer adjacent to the upstream surface of the sphere is reduced. The increased velocity of the fluid passing the sphere causes the fluid in the immediate vicinity of the heated layer to be dragged downstream so that the streamlines are shifted from the upstream region of the flow field.

Figures 4 and 5 show the distribution of the isotherms around the sphere at Grashof numbers of 0.05 and 25, for a Prandtl number of 0.72. As is to be expected, an increase in the Grashof number causes the thickness of the heated layer over the upstream region of the solid sphere to decrease, while that over the downstream region increases.

Figures 6 and 7 show the distribution of vorticity around the solid sphere at Grashof numbers of 0.05 and 25 for a Prandtl number of 0.72, respectively. It is seen that as the Grashof number increases, the effects of convection on the vorticity distribution become important and the contours are displaced in the downstream direction.

Figure 8 shows the variation of the surface vorticity with angle, θ, for different Grashof numbers at a Prandtl number of 0.72. The symmetrical distribution of surface vorticity confirms that even at a Grashof number of 25, diffusion is the dominant mode of vorticity transport close to the sphere surface.

The variation of surface pressure with angle, θ, for different Grashof numbers at a Prandtl number of 0.72 is shown in Fig. 9. It is seen that as the Grashof number increases, the surface pressure over the upstream region of the sphere increases while that over the downstream region decreases and exhibits a shallow minimum.

The variation of local Nusselt number with angle for different Grashof numbers at a Prandtl number of 0.72 is shown in Fig. 10. It is seen that as the Grashof number increases, the Nusselt numbers over the upstream region of the sphere increase while the local Nusselt numbers over the downstream region decrease.

Figure 11 shows the variation of average Nusselt number with Grashof number. In this figure the analytical result of Hossain [4] and the experimental

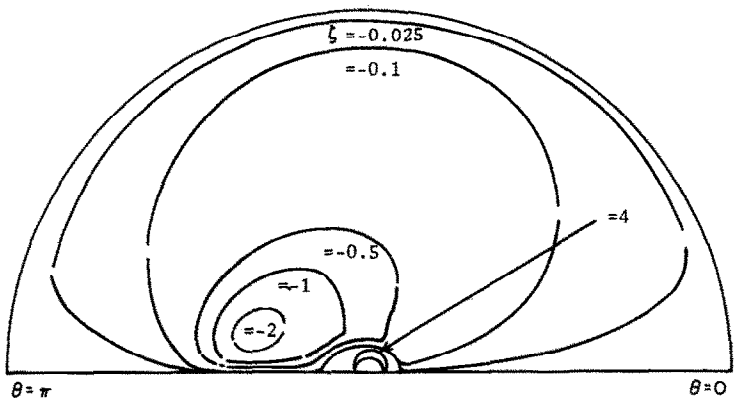

FIG. 7. Vorticity distribution, $Gr = 25$, $Pr = 0.72$.

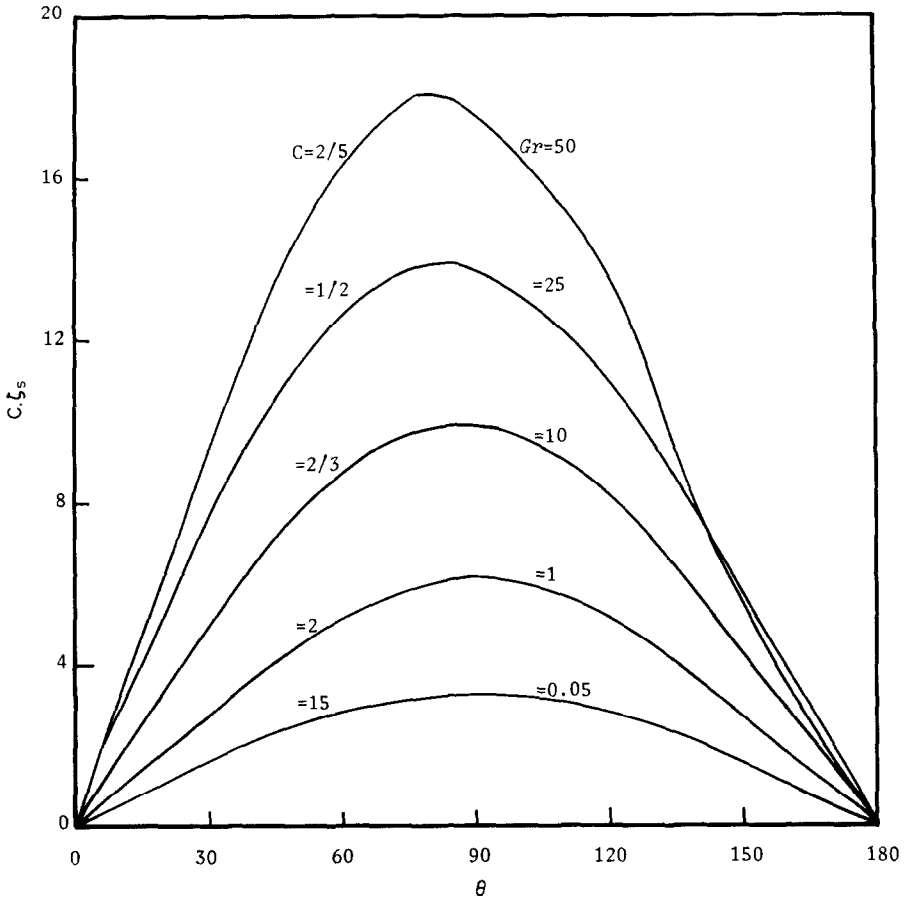

FIG. 8. Variation of surface vorticity with Gr, $Pr = 0.72$.

results of Mathers, Madden and Piret [8], Tsubouchi and Sato [9] and Yuge [10] are also plotted for comparison purposes. It is seen that the present solutions predict lower values of the average Nusselt number than the experimental measurements. This could be attributed to the fact that most experimental measurements of free convective heat transfer are subject to disturbances in the fluid caused by external factors and to additional heat losses because of conduction and radiation. These factors lead to overestimates of the average Nusselt numbers.

It may be concluded that on the basis of the above discussion the numerical solutions obtained are physically realistic.

REFERENCES

1. D. V. Pandya, Free convective heat and mass transfer from spheroids, elliptic cylinders and similarity flow bodies, Ph.D. Thesis, London University (1967).
2. J. J. Mahony, Heat transfer at small Grashof numbers, *Proc. R. Soc., London* **A238,** 412–423 (1956).
3. F. E. Fendel, Laminar natural convection about an isothermally heated sphere at small Grashof numbers, *J. Fluid Mech.* **34,** 163–176 (1968).
4. M. A. Hossain, Laminar free convection about an isothermal sphere at extremely small Grashof numbers, Ph.D. Thesis, Cornell University (1966).
5. P. Meyer, Heat transfer to small Grashof particles by natural convection, *Inst. Chem. Engrs* **15,** 127–130 (1937).
6. W. Elenbaas. The dissipation of heat by free convection from sphere and horizontal cylinders, *Physica* **9,** 285–296 (1942).
7. W. E. Ranz and W. R. Marshall, Jr., Evaporation from drops, *Chem. Engng Prog.* **48,** 173–180 (1952).
8. W. G. Mathers, A. J. Madden, Jr. and E. L. Piret, Simultaneous heat and mass transfer in free convection, *Ind. Engng Chem.* **49,** 961–968 (1957).
9. T. Tsubouchi and S. Sato, Heat Transfer from fine wires and particles by natural convection, res. of the Inst. of High speed Mech., Tohoku Univ. **12,** 127–132 (1960).
10. T. Yuge, Experiments on heat transfer from spheres including combined natural and forced convection, *Trans. ASME* **C82,** 214–220 (1960).
11. G. K. Batchelor, *An Introduction to Fluid Dynamics*, Chaprs 2–5. Cambridge University Press, Cambridge (1970).
12. G. D. Smith, *Numerical Solution of Partial Differential Equations*, Chaprs 2 and 5. Oxford University Press, London (1965).
13. R. D. Richtmyer and K. W. Morton, *Difference Methods for Initial Value Problems*, 2nd edn Chap. 1. John Wiley, New York (1967).
14. P. J. Roache, *Computational Fluid Dynamics*, Chap. 3. Hermosa, Albuqurque (1972).
15. T. M. Soo, A numerical solution of the Navier–Stokes

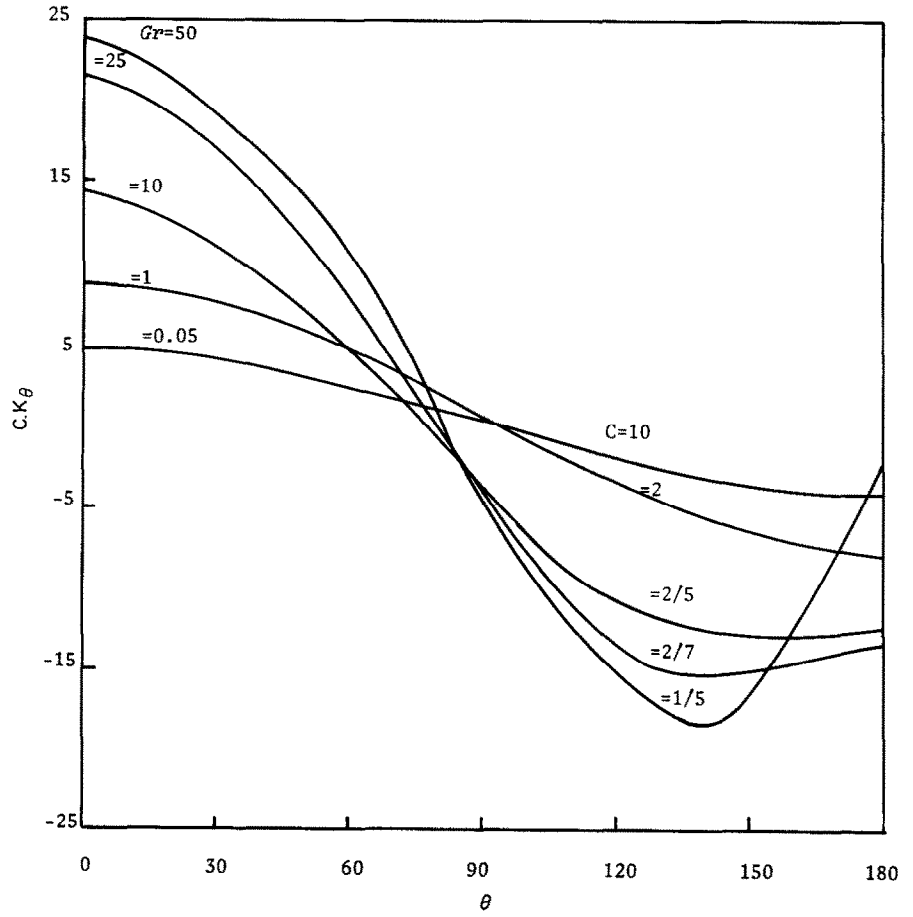

FIG. 9. Variation of surface pressure with Gr, $Pr = 0.72$.

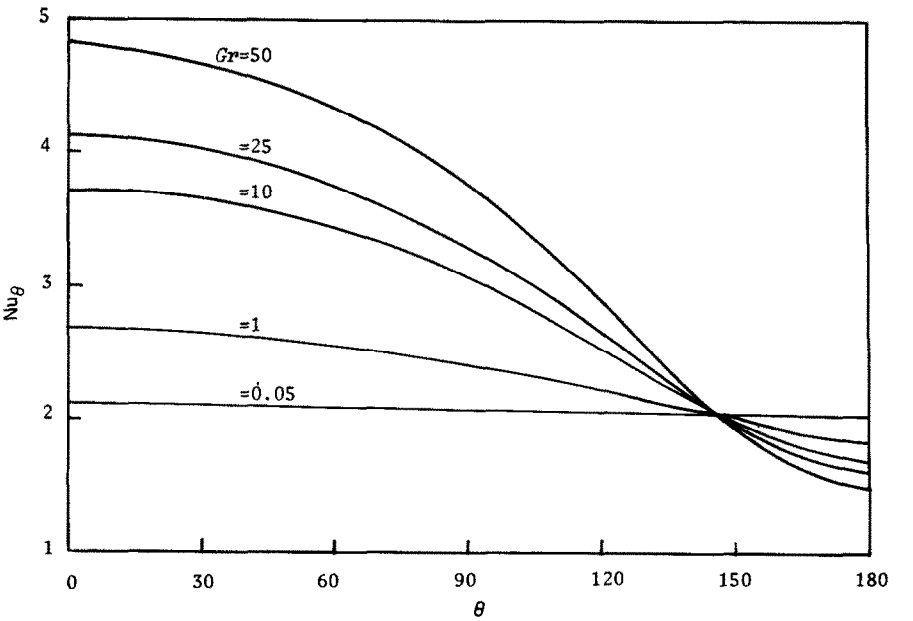

FIG. 10. Variation of local Nusselt number with Gr, $Pr = 0.72$.

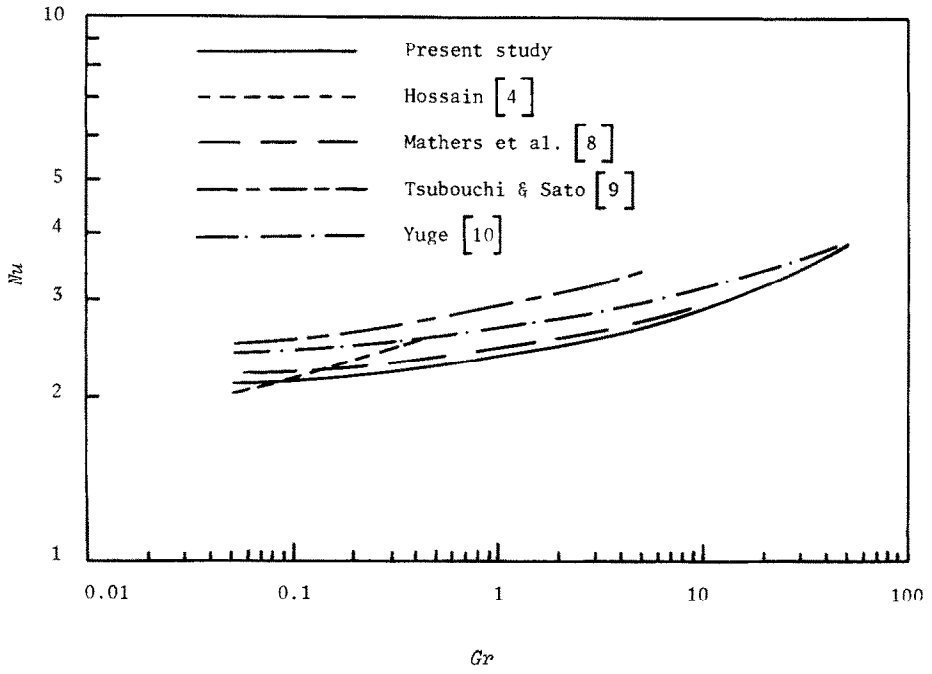

FIG. 11. Comparison of average Nusselt numbers, $Pr = 0.72$.

and diffusion equations for two equally sized spheres, Ph.D. Thesis, London University (1976).
16. J. Hellums, Finite difference computation of natural convection, Ph.D. Thesis, Michigan University (1961).
17. K. Rafique, Digital simulation of viscous incompressible flow around a solid sphere, Ph.D. Thesis, London University (1971).
18. D. B. Spalding, A. D. Gosman and L. S. Caretto, Removal of an instability in a free convective problem. Report EF/TN/A/35 Mechanical Engineering Department, Imperial College of Science and Technology, London (1971).
19. A. D. Gosman, W. W. Pun, A. K. Runchal, D. B. Spalding and M. Wolfshtein, *Heat and Mass Transfer in Recirculating Flow*. Academic Press, London (1969).

RESOLUTION NUMERIQUE DE LA CONVECTION THERMIQUE PERMANENTE ET NATURELLE AUTOUR D'UNE SPHERE SOLIDE

Résumé—On étudie numériquement le transfert thermique par convection naturelle permanente d'une sphère solide pour un fluide newtonien incompressible avec des nombres de Grashof de 0,05, 1, 10, 25 et 50, un nombre de Prandtl de 0,72. Les équations de la fonction de courant, de l'énergie et de la vorticité sont résolus en utilisant une méthode extrapolée de Gauss–Seidel. Les valeurs obtenues pour le nombre de Nusselt moyen sont en accord raisonnable avec les mesures expérimentales. On observe aussi que la méthode utilisée ne peut pas être appliquée à la recherche des solutions pour un nombre de Grashof supérieur à 50.

NUMERISCHE LÖSUNG FÜR DIE STATIONÄRE WÄRMEABGAEBE EINER KUGEL BEI FREIER KONVEKTION

Zusammenfassung—Es wurde eine theoretische Untersuchung der Wärmeabgabe bei stationärer freier Konvektion einer Kugel an ein inkompressibles newton'sches Fluid bei Grashof-Zahlen von 0,05; 1; 10; 25 und 50 und bei einer Prandtl-Zahl von 0,72 durchgeführt. Die Stromfunktion sowie die Energie- und Wirbeltransportgleichungen wurden mit einem extrapolierten Gauss-Seidel-Verfahrengelöst. Die berechneten Werte der mittleren Nusselt-Zahl stimmen mit Meßwerten aus früheren Veröffentlichungen anderer Forscher gut überein. Es wurde auch festgestellt, daß diese Methode für Grashof-Zahlen über 50 nicht anwendbar ist.

ЧИСЛЕННОЕ ИССЛЕДОВАНИЕ СТАЦИОНАРНОГО СВОБОДНОКОНВЕКТИВНОГО ТЕПЛОПЕРЕНОСА ОТ ТВЕРДОЙ ПОВЕРХНОСТИ

Аннотация — Проведено численное исследование стационарного свободноконвективного теплопереноса от твердой сферы к несжимаемой ньютоновской жидкости при значениях числа Грасгофа, равных 0,05; 1; 10; 25 и 50, и числа Прандтля, равного 0,72. Уравнения функции тока, сохранения энергии и завихренности решались модифицированным методом Гаусса-Зейделя. Полученные значения среднего числа Нуссельта хорошо согласуются с результатами экспериментальных измерений, проведенных другими исследователями. Очевидно, что используемый метод нельзя применять для нахождения решений при значениях числа Грасгофа, превышающих 50.